CONFERENCE PRE-PRINT

TOKAMAK ENERGY'S HIGH TEMPERATURE SUPERCONDUCTING MAGNET FUSION POWER PLANT CONCEPT

Developed under the U.S. Department of Energy Milestone-Based Fusion Development Program

S.A.M. McNAMARA, J. ASTBURY, N. LOPEZ, X. ZHANG, A. ALIEVA, M. BORSCZ, E. MAARTENSSON, S. MEDVEDEV, M. ROBINSON, A. SCARABOSIO, M. SCARPARI, Y. TAKASE, J. WILLIS, C. WILSON, E. YILDIRIM, THE TOKAMAK ENERGY MILESTONE PROGRAM TEAM AND COLLABORATORS Tokamak Energy Ltd

Oxfordshire, United Kingdom

Email: steven.mcnamara@tokamakenergy.com

Abstract

As part of the U.S. Department of Energy's Milestone-Based Fusion Development Program, Tokamak Energy is working with collaborators from U.S National Laboratories, Universities and companies to deliver a pre-conceptual design for a fusion power plant and a set of associated technology development roadmaps. This manuscript summarises the progress towards this pre-conceptual design with a particular focus on major design decisions and their impact on the final integrated design. By allowing physics and engineering design efforts and market analysis to progress in parallel, the candidate design space identified is inherently one of compromise. Some of these considerations are highlighted here, such as the radial build, plant economics, and impact of aspect ratio. Ongoing higher-fidelity physics modelling to further explore the candidate design space and identify optimal design choices is also discussed.

1. INTRODUCTION

Tokamak-based power plant concepts can be broadly divided into those targeting pulsed or steady-state plasma operating regimes. In pulsed devices, a fraction of the plasma current is driven inductively and the device operates in repeated cycles. Pulse lengths can vary significantly between tens of minutes to several hours. Pulsed operating regimes tend to allow for higher plasma currents, offering a direct way to achieve the necessary plasma confinement. However, the higher plasma current makes the plasma susceptible to low-order tearing modes and increases the severity of unmitigated plasma disruptions. Pulsed operation also imposes significant challenges for plant integration: cyclic thermal and electromagnetic loads reduce component lifetimes and increase operational costs, increased disruption severity requires robust avoidance of unmitigated disruptions, and capacity factor is lowered due to downtime between pulses. Thermal storage can be used as a buffer between the pulsed fusion power output and the power conversion system allowing for continuous delivery of electrical power to the grid.

Steady-state operating points are highly coupled due to the need for high bootstrap current fractions, and as a result, performance is strongly dependent on plasma confinement and stability. Regimes that offer the potential for enhanced confinement and improved stability are, therefore, attractive candidates for steady-state operation. The most promising concepts are the spherical tokamak (ST) and advanced tokamak (AT). Both concepts share many features, including strong plasma shaping, broad current profiles, low or reversed magnetic shear, high edge safety factor, elevated minimum safety factor to avoid sawteeth and low-order NTMs, and active stability control. They also look to exploit synergies between plasma turbulence suppression, MHD stability and high bootstrap current and pressure profiles.

This manuscript explores the design space for a steady-state tokamak fusion power plant, discusses some of the key design constraints and identifies potentially attractive operating regimes. A workflow for assessing and down-selecting design concepts has been developed and starts with the identification of promising design points using an in-house whole-plant systems modelling code, PyTok, which scans over a wide range of potential device parameters and allows the sensitivity of input assumptions and models to be evaluated. PyTok includes simplified models for all of the major plant systems, parametric CAD

generation for cost modelling and neutronics assessments, large parameter space optimisation and sensitivity studies. Promising design points are then taken forward for further assessment using a series of integrated physics and engineering workflows with increasing fidelity. At the pre-conceptual design stage the focus has been on exploring the design space, identifying and understanding the key design trade-offs, and taking the major decisions that define the high-level plant concept. The emphasis has been on identifying attractive design spaces, rather than optimising a single design point, and selecting selecting design choices that are complementary and benefit the overall plant performance.

2. KEY DESIGN DECISIONS AND THEIR IMPACT ON THE INTEGRATED DESIGN

This section discusses some of the main trade-offs and driving factors that have influenced the device design. The results presented were generated using the PyTok whole plant systems modelling code.

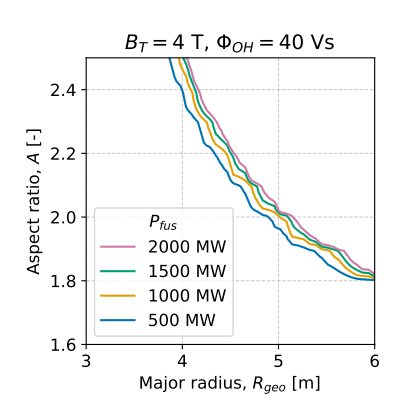
2.1. Inboard radial build: balancing component lifetime, toroidal field strength, and solenoid capacity

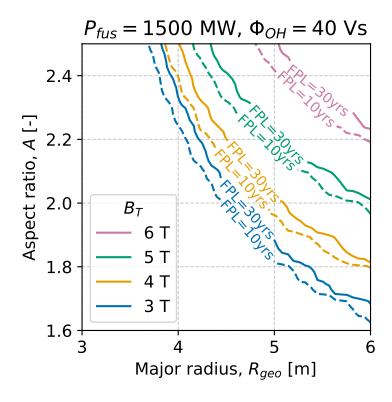
A critical design consideration for all tokamaks is the inboard radial build, which sets the scales for the overall device dimensions. In a pilot or power plant this area must, at a minimum, contain the inner leg of the toroidal field (TF) coils and any associated supporting structures and cryogenic cooling infrastructure; radiation shielding; and plasma-facing components. Depending on the wider device design, it may also contain a central solenoid and/or inboard tritium breeding.

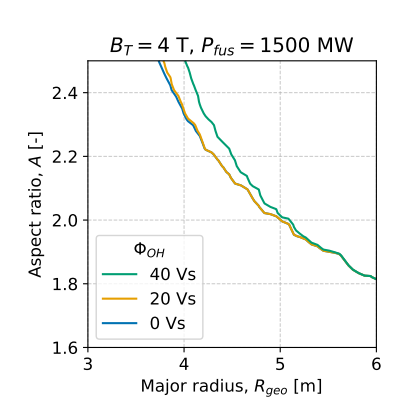
Some of the major decisions taken in this project and their impact on the design of the inboard region are:

- Natural lithium as the tritium breeding medium. Potential breeding media include pure lithium, lithium lead, lithium oxide, lithium-bearing ceramics, and FLiBe. Each medium has a different level of lithium-6 enrichment, ranging from natural to highly enriched, that impacts the achievable tritium breeding ratio (TBR) and energy multiplication of the blanket. Among these options, natural lithium has one of the highest volumetric tritium breeding ratios and an energy multiplication factor of ~ 1.15 and does not require the development of an end-to-end, fusion-compatible lithium-6 enrichment supply chain. It does however restrict the choice of coolants, as discussed below.
- No inboard tritium breeding. Achieving tritium self-sufficiency is a key requirement for commercial fusion. Even pre-commercial devices should have a TBR approaching or exceeding 1 due to the cost and availability of tritium. The need for inboard tritium breeding is determined by the target TBR, the choice of breeding medium and the machine parameters. The high volumetric TBR of natural lithium allows TBR ≥ 1.15 without inboard breeding at aspect ratios up to $A \sim 2.3$.
- Helium as the centre column shield coolant. Typical cooling fluids considered in the tokamak core are water, helium
 and carbon-dioxide. Although water is an efficient coolant and has the added benefit of contributing to shielding due
 to its neutron moderating properties, its high chemical reactivity with metallic lithium makes it an incompatible choice
 with the selected breeding medium. Choosing helium instead, however, increases the thickness of the centre column
 shielding required to achieve the same magnet lifetime, therefore increasing the overall device dimensions.
- Lifetime toroidal field coils. The inboard region of the device is subject to intense neutron irradiation that will degrade the performance of components such that they require periodic replacement. The plasma facing components and at least part of the central column shield will require replacement during the plant's operational life. The inner shield (furthest from the plasma) and any other components inboard of this (the toroidal field coil legs and central solenoid) may be designed as lifetime or replaceable components. Replacing HTS TF coils would require either developing deand re-mountable low-resistance joints or disassembling the majority of the machine, along with developing the associated maintenance schemes. Both approaches would likely increase the cost and/or required maintenance downtime, negatively impacting the operational costs and/or availability. It was therefore decided that the TF magnets would be lifetime components, with a target full power life (FPL) of 30 years.
- Solenoid to assist with ramp-up to flattop operating point. While steady-state operating regimes do not require ohmic current drive during flattop, the inclusion of a reasonably sized solenoid has several benefits. Firstly, it alleviates risk associated with extrapolating solenoid-free research results to a high current, high performance pilot or power plant regime for the first time. Secondly, it reduces the time taken to ramp-up to the flattop operating point, thereby reducing the time the plant is consuming electrical power, rather than generating it. Thirdly, during commissioning or demonstration phases of the plant operational cycle it is also beneficial to have the ability to drive ohmic current during the flat-top phase. Finally, it allows for rapid control of the plasma current during the flat-top phase in the event of any deviations from the target value. The potential for solenoid recharge during the approach to burning conditions [1] offers a way to increase the available solenoid flux.

Using these design choices, a subset of the PyTok modules were used to investigate the impact of fusion power, TF strength and solenoid flux on the TF coil lifetime. Note, this section does not include any other considerations, such as the whether a plasma exists that can produce the specified fusion power. This is considered in a later section. For the radial build, PyTok uses a simplified representation of Tokamak Energy's toroidal field coil winding pack configuration and real engineering parameters to construct an annular region in the centre column that has sufficient superconducting material to carry the current required to produce the field, enough thermal mass to provide quench protection, and a steel case thick enough to withstand the stress induced by the electromagnetic forces. If included, the annulus wraps around the solenoid, the outer diameter of which is calculated based on the required bipolar flux swing on the plasma. The space between the outer diameter of the superconducting core and the plasma includes insulating layers, a vacuum vessel, radiation shielding and plasma facing components. The thickness of the radiation shield is varied to fill the available space. Each of the materials between the plasma and magnet system has a half-value layer (HVL), the thickness of a given material required to reduce the incident radiation intensity to 50%, derived from radiation transport simulations, which enables PyTok to estimate the total attenuation of the first wall neutron flux through the layers. The transmitted fast ($E_n > 0.1 \text{ MeV}$) neutron flux is used to calculate the degradation rate of the superconducting material, which determines the lifetime of the tokamak.







(a) Contours of 30 year full power life with varying fusion power, P_{fus}

(b) Contours of 10 and 30 year full power life with varying toroidal field, B_T

(c) Contours of 30 year full power life with varying solenoid flux, Φ_{OH}

FIG. 1. Toroidal field coil full power life (FPL) as a function of major radius and aspect ratio with varying fusion power, toroidal magnetic field and solenoid flux.

The dependence of the TF coil lifetime on the fusion power is shown in FIG.3a. The dominant factor determining the TF coil lifetime is the thickness of the inboard radiation shield. The shield has an averaged HVL of approximately 5cm, meaning a modest change in thickness has a significant impact on the TF coil lifetime. This can be seen by the close grouping of the 30-year FPL contours with changing fusion power, where increasing fusion power from 500 to 2000 MW only requires increasing the device major radius by approximately 20cm. This can be used to set the major radius of the device as a function of aspect ratio (from a centre column build perspective only). This size range also gives an indication of the device cost, which can be used to give an indication of an acceptable target fusion power range.

The dependence of the TF coil lifetime on the TF strength is shown in FIG.3b. This plot shows two interesting features. First, increasing the TF coil FPL from 10 to 30 years only requires a modest increase in major radius, again due to the short exponential attenuation length of the centre column shield. This was a contributing factor to the decision to make the TF coils a lifetime component. Second, of the three parameters plotted, the TF strength is the dominant factor in determining the device size. From the perspective of the inboard radial build alone, lower toroidal field allows for more compact devices, but this analysis does not consider if this is consistent with the wider device, particularly the plasma.

The dependence on the solenoid flux is more complex. The solenoid flux is determined by both the space available for the solenoid, which is largely determined by the TF coil build, and the solenoid coil engineering. The radial build is driven by several considerations. The cross-sectional area of the TF winding pack is determined by the amount of copper required for quench protection. Each limb is modelled as a series of rectangles representing sections of the winding pack; their number and configuration is then varied to maximise the packing efficiency in the available space. For higher magnetic fields, the cross-sectional area requirement determines the inner radius of the TF winding pack. At lower magnetic fields the TF winding pack inboard radius is set by a stress limit determined by the thickness of the steel case between the solenoid and the winding pack. (Where there is no solenoid, the winding pack moves radial inwards until it reaches the quench protection limit.) This explains why the 0 Vs and 20 Vs contours are overlapping in FIG.3c. For these cases the space available for the solenoid as determined by the TF coil build is sufficient to accommodate a solenoid of up to 20 Vs. The larger 40 Vs solenoid, however, would not fit in this space; instead, the solenoid determines the radial build by setting the inboard radius of the TF winding

pack, reducing the TF coil FPL (or requiring an increased major radius for the same FPL).

2.2. Fusion performance and economics

For fusion power to be widely adopted it must be commercially viable, offering cost competitive power and robust delivery. Early plants need not necessarily satisfy this requirement but must be economically sustainable with, for example, additional subsidies, low interest loans, tax credits or other supporting financial measures supported by governments who are also motivated by energy security and clean energy policies. There are many potential routes to fusion commercialisation with different timelines, device roadmaps, risk appetites, financing requirements and delivery models. Each have their merits, and no universal optimum path exists, with each organisation choosing how to balance the many competing factors. For an interesting discussion on pathways to fusion see [2]. While no universal trends exists, public programs have tended to follow a more "evidence driven" route, favouring more devices and robust understanding prior to deployment, whereas private companies have tended towards a "schedule driven" approach prioritising as soon as practical demonstration of commercial fusion within the bounds of available funding, regulatory compliance, and readiness of feasible technologies.

When the DOE Milestone Program was established the target was to produce a fusion pilot plant that met or exceeded the requirements described in the 2021 National Academies of Sciences, Engineering, and Medicine (NASEM) report Bringing Fusion to the U.S. Grid [3], which included: i) continuous net electricity generation of ≥ 50 MWe for at least 3 hours, ii) a tritium breeding ratio $\gtrsim 0.9$, iii) the demonstration of operations through several environmental cycles, and iv) to be built with an overnight capital cost of < \$5 Bn (in 2021 dollars, which is equivalent to $\sim \$6$ Bn in 2025). Such a mission is perhaps appropriate for a public program or a program with significant public sector financial support, however, for a privately led program delivered with majority private equity it is a challenging design space due to high cost and limited potential for commercial output. For any project to be successful it must be both technically deliverable and financeable. For privately funded devices, capital markets appear willing to accept the increased risk of increasing the scope from a pilot plant towards a first of a kind power plant in return for significantly increased upside potential. The mission for this program has therefore deviated from that defined in the NASEM report to include commercially competitive net power generation and availability targets. These include net electric power output of 800 - 1000 MWe at 80% availability averaged over a 30 year full power life, the demonstration of a closed-loop tritium fuel cycle with a commercially representative inventory and doubling time, and a First of A Kind (FOAK) installed capacity cost of < \$12000/kWe. These modified targets are included alongside the need to retire all necessary risks on the path to commercially relevant operations, therefore the device will be sized to allow two distinct operating phases, a pilot plant phase, where key technologies are demonstrated at low integrated performance, and a power plant phase, targeting economically sustainable operations. Due to the low readiness of fusion technologies and the lack of industrial experience in constructing and operating fusion power plants, any cost estimates will be highly uncertain and should be interpreted with care. However, it is important for fusion developers to consider the economics of proposed solutions. The results presented here then are intended to inform the general design direction by showing important trends and not to be taken as reliable estimates at this stage.

The general trend of net electric power output as a function of Overnight Capital Cost (OCC) for the power plant phase using FOAK costings is illustrated in FIG.2. The data was generated by performing a large ensemble parameter space scan using PyTok. For these particular scans, for a given data point, PyTok uses an optimisation routine where it attempts to match a target value of fusion power whilst remaining below specified values of the ratio of normalised beta, β_N , to a scaling for the no-wall stability limit, $C_{\beta_N} = \beta_N/\beta_{N, \text{ no-wall}}$, a similar ratio for poloidal beta, C_{β_p} , which is discussed in more detail in a later section, the Greenwald density fraction, f_{GW} , and a simple divertor power handling metric, P/R, which can be satisfied by varying the effective ion charge, Z_{eff} , and corresponding radiated power. The optimiser is not always successful as an operating point that satisfies all the target parameters may not exist. These points can be filtered from the final dataset and allows the impact of these stability limits to be determined. The ensemble scan uses the quasi-random Sobol sampling method to scan over the device geometry, magnetic field, and target fusion power. These scans were performed for different values of the radiation corrected energy confinement enhancement factor (H-factor) relative to the ITER98(y,2) scaling, H98*. All other assumptions and inputs were held constant across the scan. The full dataset is plotted along with a trend line representing the optimised design points.

Three key features can be seen in the data. Firstly, since fusion requires a lot of ancillary systems and has high recirculating power requirements, the capital cost of the plant equipment required to balance the recirculating power is significant. The incremental cost required to produce positive $P_{elec,net}$ is relatively modest compared to this. This only considers economics and does not include any risk consideration or the potentially differing requirements of a low power demonstrator compared to a high power commercial plant.

Secondly, the plant performance is strongly dependent on the assumed plasma energy confinement enhancement factor. Steady-state operating points are highly coupled due to the need for high bootstrap current fractions, and as a result, performance is

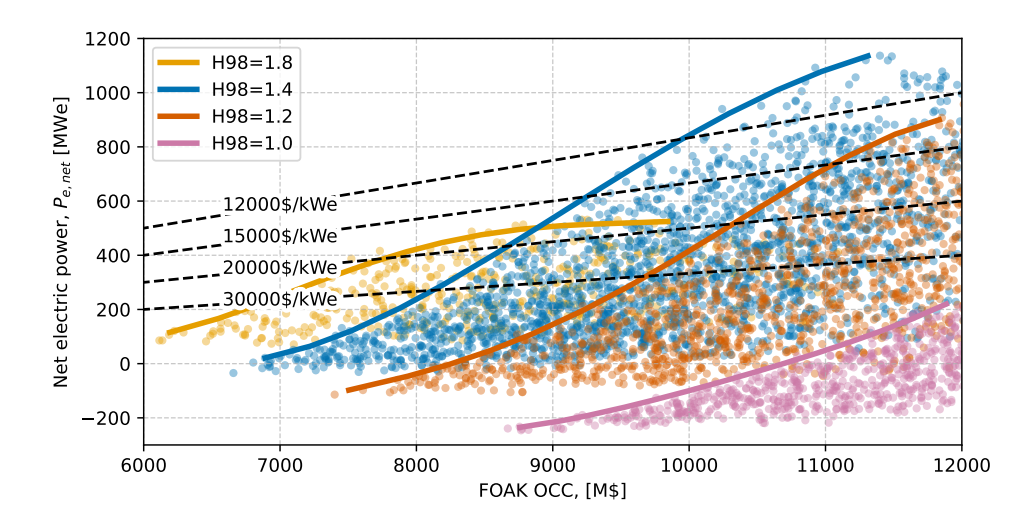


FIG. 2. Net electric power, $P_{e,net}$ as a function of Overnight Capital Cost, OCC, for different radiation corrected energy confinement enhancement factor relative to the ITER98(y,2) scaling.

more strongly dependent on confinement than in inductively driven plasmas. Thirdly, the highest energy confinement does not always correspond to the lowest installed capacity cost, as shown by the trend of the H98=1.8 curve. This may at first seem counter intuitive, but can be explained by the fact that H-factor determines the amount of fusion power required to reach a certain fusion gain, with higher H-factors requiring lower fusion powers. As H-factor increases, there comes a point where the plasma ignites (or reaches the maximum allowable fusion gain) and it is not possible to increase fusion power further, without degrading confinement.

2.3. Design space scoping

Based on the the requirements for the power plant phase a device major radius of $R_{geo}=5$ m was chosen for this preconceptual design study. Given uncertainties, this isn't optimised but is approximately the size required to achieve acceptable performance in the power plant phase. The remainder of the pre-conceptual design was mainly focused on the pilot operating phase, which was targeting a net electric power in the range 300-400 MWe. Accounting for all assumptions, this was found to correspond to a fusion power of around 1500 MW. For the pre-concept design it was useful to fix this early in the design process to allow balance of plant systems to be appropriately sized and for their design to progress. For fixed values of fusion power and solenoid flux, a PyTok scan was performed to determine the impact on the design space of varying major radius, aspect ratio and toroidal magnetic field. In this scan all other input parameters and assumptions were held constant. Contours of net electric power, $P_{e,net}$ as a function of major radius and aspect ratio for different toroidal magnet fields are plotted in FIG.3. A contour showing where the TF magnet full power life is 30 years and contours of the ratio of $C_{\beta N}=\beta_N/\beta_{N,\ no-wall}$ are also shown. The radiation corrected energy confinement enhancement factor relative to the ITER98(y,2) scaling is 1.4 in all plots and the simple divertor exhaust metric $P/R \le 25$ MW/m.

For fixed major radius a series of design points at different magnetic fields and aspect ratios is shown in Table.1. The three design points shown produce similar levels of net power and comparable FOAK ONC. At fixed major radius and TF full power life, reducing aspect ratio requires the toroidal field to be reduced and the plasma current increased. At fixed major radius, as aspect ratio is reduced the plasma operating point moves closer to the no-wall β_N limit. Had R_{geo} been allowed to change slightly it would have been possible to fix other parameters in the scan, for example $P_{e,net}$. Reducing H98* means more H&CD power is required to reach the target fusion power, reducing the net electric power to below the target and increasing the ONC.

As shown, with the simplified assumptions used in the whole plant modelling, there is a relatively broad range of integrated device designs that produce equivalent overall plant performance. The next step in the device design is to go beyond this simplified modelling to determine regions in this parameter space that are likely to yield the highest performance. A major factor in this is the plasma performance, which has a significant impact on the overall device performance. A key question then, is how the achievable plasma performance varies across the acceptable engineering design space.

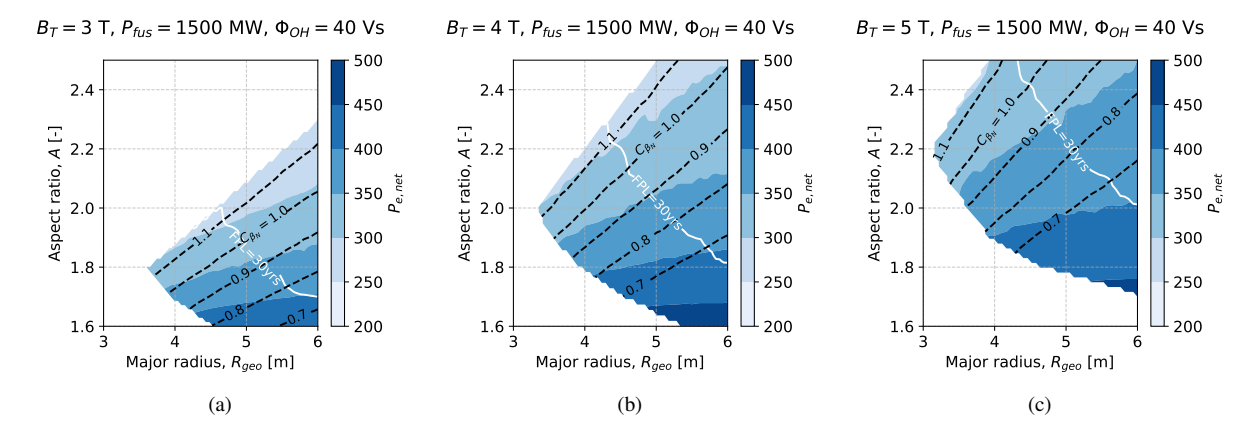


FIG. 3. Net electric power as function of major radius and aspect ratio. The FPL= 30 years contour is shown in white and contours of normalised beta relative to a scaling for the no-wall limit as dashed black lines.

	$H98^* = 1.4$			$H98^* = 1.2$		
Toroidal field [T]	3.0	4.0	5.0	3.0	4.0	5.0
Major radius [m]	5.0	5.0	5.0	5.0	5.0	5.0
Aspect ratio [-]	1.9	2.05	2.25	1.9	2.05	2.25
Plasma current [MA]	19.6	18.0	16.2	20.1	18.4	16.4
Fusion power [MW]	1450	1485	1485	1490	1500	1500
Heating & Current Drive Power [MW]	125	120	115	195	185	175
Fusion gain [-]	11.5	12.6	13.2	7.6	8.2	8.5
Net electric [MWe]	320	350	360	220	250	260
No-wall β_N limit ratio, C_{β_N} [-]	1.0	0.88	0.85	0.93	0.81	0.78
FOAK ONC [M\$]	9,100	9,700	10,300	10,200	10,700	11,300

TABLE 1. Whole plant system modelling design space for different radiation corrected confinement assumptions. All design points have a TF full power life of 30 years and a simple power exhaust metric of P/R = 25 MW/m.

3. PLASMA DESIGN ASSESSMENT

Promising design points are then taken forward for further assessment using a series of integrated physics and engineering workflows with increasing fidelity. A series of reference flat top operating points and scenarios are developed and further assessed for MHD stability, heating and current drive (H&CD) scoping, turbulence and transport analysis, pedestal stability, scrape-off layer and divertor modelling, free-boundary equilibrium evolution and optimisation of the poloidal field coil system. Note, as the pre-concept design is still evolving not all the work presented in this section is based on the same reference design points.

3.1. Flat-top operating points

Reference flat top operating points are developed using 1.5D transport and equilibrium codes (ASTRA [4] and FUSE [5]) to integrate various simplified models and produce plasma equilibrium and radial profiles that can be used for further assessment. The plasma kinetic profiles can be either specified or estimated using a Bohm/gyro-Bohm analytic transport model [6], and are scaled to match the target fusion power and Greenwald density fraction. The flat top operating points use electron cyclotron (EC) H&CD with a prescribed deposition profile and current drive efficiency. The current profile is tailored to optimise the safety factor profile to maintain $q_{min} \geq 2.2$ to avoid neo-classical tearing modes and infernal modes. For the pedestal, either the FUSE EPED-NN or a simplified expression for the height and width [7], which allows for different height and width coefficients to be tested and different width-height relationships (e.g. DIII-D like, where the pedestal width scales with the pedestal-top poloidal beta as, $w_{ped} \sim \beta_{p,ped}^{0.5}$ or NSTX like, where $w_{ped} \sim \beta_{p,ped}^{1.0}$ are used.

3.2. Plasma operating scenario

An initial definition of the plasma operating scenario is developed using METIS, a fast integrated tokamak modelling tool for scenario design [8]. This allows candidate scenarios to be explored and provides an initial estimation of the poloidal flux

required to reach and sustain the target plasma current and the contributions from the solenoid and poloidal field coils. To convert the fixed-boundary equilibrium used in METIS to free-boundary equilibrium, METIS has been loosely coupled to the FreeGS free-boundary equilibrium code¹. The time evolution of the free-boundary equilibrium is used as input to a magnet optimisation code, SCOPE, which, respecting engineering constraints, finds optimum poloidal field coil locations and currents for a large ensemble of operating points and scenarios.

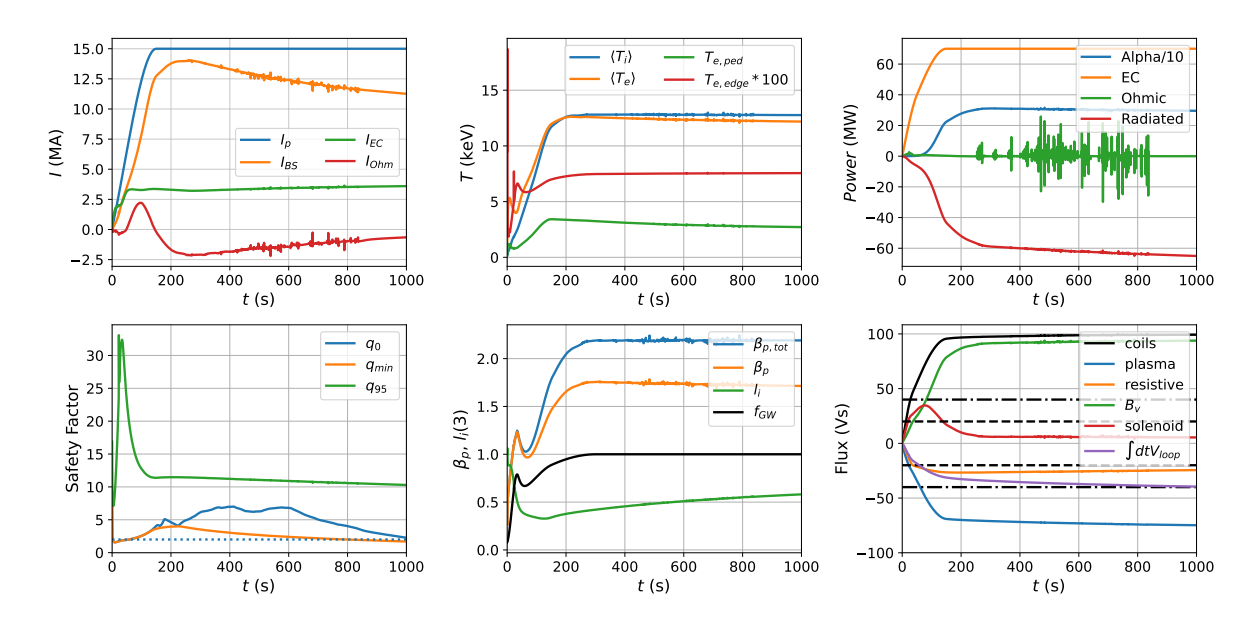


FIG. 4. Reference plasma operating scenario showing the ramp-up and beginning of the flat-top phase.

A reference operating scenario is shown in FIG.4. The plasma is evolved from a lower single null equilibrium to a full bore double null flat-top configuration. The plasma current ramp takes 150 seconds to reach the flat-top current of 15 MA. During the transition to burn, the increase in β_p driven by the increase alpha heating, and the corresponding increase in the vertical field required to maintain the plasma equilibrium cause the plasma current to be overdriven, allowing for a partial recharge of the central solenoid.

3.3. Heating & current drive

Presently, an auxiliary heating & current drive (H&CD) system consisting of electron cyclotron (EC) H&CD for ramp-up and flat-top along with ion cyclotron (IC) heating to provide direct ion heating to assist with fusion ignition during ramp-up is being considered, but EC-only scenarios are also being developed. The initial design of the EC system for ramp-up and flat-top has been developed using a computationally efficient physics-based optimisation framework [9], although more traditional scoping methods (i.e. parametric scans with ray-tracing codes) were also used for early design points [10]. For the flat top operating points, fundamental O-mode with frequencies between 160-200 GHz is accessible, fully absorbed, and found to give the highest current drive efficiencies of $\gtrsim 50$ kA/MW. The launchers are positioned on the low field side between the midplane and x-point (low-field side top-launch), and directed such that deposition occurs on the high field side of the magnetic axis to minimise trapped particle effects. The IC system for ramp-up is being designed based on a He-3 minority heating scheme transitioning to second-harmonic tritium heating as the plasma temperature increases.

3.4. MHD stability

MHD stability analysis performed using the KINX ideal MHD code has identified a complicated interaction between the assumed pedestal height and width, no-wall and ideal-wall normalised beta (β_N) limits, vertical stability and proximity to a connected double null configuration. The no-wall and ideal-wall β_N limits are found to reduce with increasing pedestal height due to an increase in the edge current density. Increasing pedestal height also destabilises a n=0 mode localised near the x-points. This mode can be stabilised by toroidally conducting structures located close to the x-point or by moving away from a connected double null configuration, however this reduces the no-wall and ideal-wall β_N limits.

For high bootstrap fraction operating points it was also found that an ideal MHD external n=1 kink mode, with stability properties similar to those of the peeling-ballooning modes that limit the pedestal pressure, can set a limit on the achievable

¹https://github.com/freegs-plasma/freegs

global poloidal beta (β_p) in contrast to the classic Troyon limit for toroidal beta in the case of q_0 close to 1. For high-q equilibria only the global n=1 kink mode remains unstable while higher-n modes are stable together with localised ballooning modes due to the second stability access in a large portion of plasma volume. For $q_{min}>2$, the coupling to the global m/n=2/1, 1/1 modes, that plays an important role in the Troyon scaling realisation, is weak. That is why the no-wall β_p stability limit against global n=1 mode scales in the same manner as peeling-ballooning limits favouring strong plasma shaping with weaker dependence on pressure peaking. In turn the β_p limit restricts the achievable β_N which can be significantly lower than $\beta_N>4$ reachable in plasmas with flat pressure profile and higher global shear (higher internal inductance).

3.5. Plasma exhaust

Plasma exhaust in a relatively compact device needs careful management. Long and short leg configurations in both double null and disconnected double null (separated by more than 3 scrape-off-layer heat flux decay lengths, λ_q) are studied using the Hermes-3 1D code [11], for assessing detachment access with Argon seeding. Due to the lack of first-principle based predictions for λ_q in the relevant parameter space, the sensitivity of detachment access to λ_q are investigated, with λ_q ranging from the ion gyro-radius $\rho_i \approx 1.5$ mm to the ion poloidal gyro-radius $\rho_{i,pol} \approx 4$ mm, assuming $T_{i,sep} \approx 500$ eV. Two cases of power into the scrape-off-layer of $P_{SOL} = 150$ and 300 MW are also compared for the various configurations above. In all geometrical configurations, detachment can be achieved with scrape-off-layer Argon concentrations of $\leq 2\%$ and a separatrix density less than 5×10^{19} , except in the worst case scenario of $\lambda_q = \rho_i$ and $P_{SOL} = 300$ MW. For detachment access, double null is slightly favoured compared to single null, and long leg is slightly favoured compared to short leg, although the comparative gain is minimal. The possibility of using an x-point radiator is also being explored.

ACKNOWLEDGEMENTS

Tokamak Energy acknowledges U.S. Federal support for this work under TIA DE-SC0024889. This work was prepared as an account of work sponsored by an agency of the United States Government. Neither the United States Government nor any agency thereof, nor any of their employees, nor any of their contractors, subcontractors or their employees, makes any warranty, express or implied, or assumes any legal liability or responsibility for the accuracy, completeness, or any third party's use or the results of such use of any information, apparatus, product, or process disclosed, or represents that its use would not infringe privately owned rights. Reference herein to any specific commercial product, process, or service by trade name, trademark, manufacturer, or otherwise, does not necessarily constitute or imply its endorsement, recommendation, or favoring by the United States Government or any agency thereof or its contractors or subcontractors. The views and opinions of authors expressed herein do not necessarily state or reflect those of the United States Government or any agency thereof, its contractors or subcontractors.

REFERENCES

- [1] M Gryaznevich, VA Chuyanov, and Y Takase. "Pulsed spherical tokamak—A new approach to fusion reactors". In: *Plasma* 5.2 (2022), pp. 247–257.
- [2] IT Chapman, T Bestwick, and P Methven. "Public-private partnership in the UK fusion program". In: *Physics of Plasmas* 30.10 (2023).
- [3] RJ Hawryluk et al. "Bringing fusion to the us grid". In: *The National Academies of Science Engineering and Medicine NASEM Public Briefing February* 17 (2021), p. 2021.
- [4] Gregorij V Pereverzev and e PN Yushmanov. "ASTRA. Automated System for TRansport Analysis in a tokamak". In: (2002).
- [5] O. Meneghini et al. "FUSE (Fusion Synthesis Engine): A Next Generation Framework for Integrated Design of Fusion Pilot Plants". In: *arXiv* (2024). DOI: 10.48550/arXiv.2409.05894.
- [6] E Tholerus et al. "Flat-top plasma operational space of the STEP power plant". In: Nuclear Fusion 64.10 (2024), p. 106030.
- [7] S Yu Medvedev et al. "Influence of plasma pedestal profiles on access to ELM-free regimes in ITER". In: *Plasma Physics Reports* 42.5 (2016), pp. 472–485.
- [8] JF Artaud et al. "Metis: a fast integrated tokamak modelling tool for scenario design". In: Nuclear Fusion 58.10 (2018), p. 105001.
- [9] NA Lopez et al. "Fast physics-based launcher optimization for electron cyclotron current drive". In: Plasma Physics and Controlled Fusion 67.5 (2025), p. 055012.
- [10] A Alieva et al. "Progress in the pre-conceptual design of the auxiliary heating and current drive system for the Tokamak Energy Fusion Pilot Plant". In: *EPJ Web of Conf.* (in press).
- [11] Ben Dudson et al. "Hermes-3: Multi-component plasma simulations with BOUT++". In: *Computer Physics Communications* 296 (2024), p. 108991.